Neuroscience 290 (2015) 570–580

THE EFFECT OF ESTROGEN-RELATED RECEPTOR α ON THE REGULATION OF ANGIOGENESIS AFTER SPINAL CORD INJURY

J. Z. HU,[a] H. LONG,[a] T.-D. WU,[a] Y. ZHOU[a] AND H.-B. LU[b]*

[a] *Department of Spine Surgery, Xiangya Hospital, Central South University, Changsha 410008, PR China*

[b] *Department of Sports Medicine, Research Center of Sports Medicine, Xiangya Hospital, Central South University, Changsha 410008, PR China*

Abstract—Estrogen receptor-related receptor-α (ERRα) is an orphan member of the nuclear receptor superfamily that interacts with peroxisome proliferator-activated receptor γ coactivator-1α (PGC-1α) to stimulate vascular endothelial growth factor (VEGF) expression and angiogenesis in a hypoxia-inducible factor-1α-independent pathway. Although it is not regulated by any natural ligand, the action of ERRα can be blocked by the synthetic molecule XCT790. In the present study, Sprague–Dawley rats were randomly allocated to a sham group, injury-saline group or injury-XCT90 group. A modified Allen's weight-drop method was applied to induce the acute traumatic spinal cord injury (SCI) model in these rats, and an injection of XCT790 was administered every 24 h, starting half an hour after the SCI contusion. Histological analyses revealed that XCT790 significantly aggravated tissue damage and decreased the number of ERRα-positive cells at 1, 3 and 7 days after SCI. Western blot and quantitative real-time polymerase chain reaction (qRT-PCR) analyses also indicated that XCT790 dramatically repressed the expression of ERRα, thus reducing the expression of VEGF and angiopoietin-2 (Ang-2) throughout the duration of the experiment, but the expression of PGC-1α was not affected. Immunofluorescence analyses indicated that vascular density and endothelial cell proliferation were decreased in the injury-XCT90 group compared with the injury-saline group. These results suggest that ERRα is involved in mediating angiogenesis after SCI in the rat traumatic SCI model.

Key words: spinal cord injury, angiogenesis, estrogen receptor-related receptor-α, XCT790.

*Corresponding author. Tel: +86-731-84327174; fax: +86-731-84327332.
E-mail address: hongbinlu@hotmail.com (H.-B. Lu).

Abbreviations: DAPI, 4',6-diamidino-2-phenylindole; EDTA, ethylenediaminetetraacetic acid; ERRE, estrogen receptor response element; ERRα, estrogen receptor-related receptor-α; HIF, hypoxia-inducible factor; IHC, immunohistochemical; PBS, phosphate-buffered saline; PGC-1α, proliferator-activated receptor γ coactivator-1α; qRT-PCR, quantitative real-time polymerase chain reaction; RT, room temperature; SCI, spinal cord injury; VEGF, vascular endothelial growth factor.

INTRODUCTION

Spinal cord injury (SCI) is the most devastating injury responsible for motor and sensory dysfunction, and it can progress to severe paraplegia and/or complications in patients. The complex pathological processes of SCI involve the original injury, a secondary lesion and spinal restoration (Amar and Levy, 1999). The primary assault causes immediate vascular disruptions at the injury epicenter (Ng et al., 2011). Subsequently, a cascade of injury responses, including astrocyte reactivity and hematogenous immune cell migration, can contribute to ischemia, necrosis, edema, apoptosis and cavitation, which then in turn contribute to further secondary damage that exacerbates the neurological deficits (Bazley et al., 2012).

It has long been understood that trauma to the spinal cord disrupts its local vasculature, resulting in petechial hemorrhage observed at the injury epicenter immediately after injury (Dray et al., 2009). Angiogenesis, the formation of new blood vessels from pre-existing vasculature, can serve to reduce the secondary damage after SCI, protecting against ischemia by increasing oxygen delivery and nutrients to sites of regeneration and removing metabolic waste (Lutton et al., 2012). Therefore, the vascular response to SCI and the molecular elements that regulate angiogenesis are critical components of SCI and repair.

Angiogenesis is a complex process in which hypoxia-inducible factor (HIF), vascular endothelial growth factor (VEGF) and angiopoietin-2 (Ang-2) are the critical ones. VEGF plays a pivotal role in the regulation of vasculogenesis, angiogenesis, remodeling, and vascular leakage under both physiological and pathological conditions (Distler et al., 2003). Activated VEGF and its receptors increase blood vessel density; restore blood flow; and promote neuronal survival, axonal regeneration and functional recovery after SCI (Long et al., 2012). Ang-2 appears to be an important signaling molecule during vascular remodeling, causing both increases and decreases in the microvascular density (Dore-Duffy and LaManna, 2007). In the presence of VEGF, the application of Ang-2 mediates an increase in capillary diameter, induces migration and proliferation of endothelial cells and stimulates the sprouting of new blood vessels. However, without sufficient VEGF, exposure to Ang-2 causes capillaries to undergo apoptotic regression (Pichiule and LaManna, 2002).

http://dx.doi.org/10.1016/j.neuroscience.2015.01.067
0306-4522/

Estrogen receptor-related receptor-α (ERRα) was one of the first identified orphan nuclear receptors that is important in the regulation of energy metabolism genes (Villena and Kralli, 2008). Similar to other transcriptional-binding sites, such as HRE (HIF response element), ERRα can activate the VEGF promoter directly through an estrogen receptor response element (ERRE) (Arany et al., 2008). As a regulator of oxidative metabolism, ERRα activity drives increased aerobic ATP production, which may support the high metabolic rate that characterizes highly proliferative cells while also increasing the cellular oxygen requirement (Stein et al., 2009). Although the expression of ERRα alone has low constitutive activity on the VEGF promoter region containing these elements, coexpression of the coactivator peroxisome proliferator-activated receptor gamma coactivator-1α (PGC-1α), strongly drives VEGF transcription (Stein et al., 2009). PGC-1α is a transcriptional co-activator that powerfully regulates cellular energy metabolism in mitochondria-rich tissues with high oxidative capacity through coactivation of the transcription factor ERRα on conserved binding sites found both in the promoter and a novel conserved enhancer located in the first intron of the VEGF gene (Arany et al., 2008; Shoag and Arany, 2010). Although regulation of VEGF through PI3Kinase/AKT and HIF is considered the classical pathway under ischemic conditions, a pathway involving ERRα and PGC-1α was recently discovered to be independent of HIF (Arany et al., 2008; Stein et al., 2008).

Although it is not regulated by any natural ligand, ERRα can be deactivated by the synthetic molecule XCT790. XCT790, which was identified as an ERRα-specific ligand and acts as an inverse agonist, not only represses the transcriptional effects of ERRα but also disrupts the interaction between ERRα and PGC-1α (Willy et al., 2004; Lanvin et al., 2007; Teyssier et al., 2008). XCT790 does not interfere with a specific proliferation-inducing pathway, allowing it to modulate the proliferation of any type of cells/tissues expressing ERRα (Bianco et al., 2009).

Our previous study suggested that HIF-1α/VEGF is involved in angiogenesis after rat SCI. However, whether ERRα also regulates angiogenesis in the traumatized SCI model remains unknown. In the present study, ERRα was investigated for its effects on PGC-1α, VEGF and Ang-2 expression, as well as vascular density and endothelial cell proliferation, in an experimental rat model of traumatic SCI by injecting animals with the inverse agonist XCT790.

EXPERIMENTAL PROCEDURES

Experimental SCI model

A total of 140 adult male Sprague–Dawley rats (200–250 g in weight) were randomly assigned into three groups: (1) sham group (n = 20); (2) injury-saline group (n = 60); and (3) injury-XCT90 group (n = 60). Each injury group was then sub-divided into three time-period sub-groups: 1, 3 and 7 days (n = 20 in each sub-group, n = 5 for each of the techniques). The animals were housed individually at a constant temperature on a 12-h light/dark cycle with free unlimited food and water. All animal care and experimental procedures were performed in accordance with protocols approved by the Laboratory Animal Users Committee at the Xiangya Hospital, Central South University, Changsha, China.

All animals were anesthetized using 10% chloral hydrate administered at 3 mg/kg intraperitoneally, and operated on under aseptic conditions. Next, a 15-mm midline skin incision was made at the thoracic region (T8–T13). A laminectomy was performed at vertebral level T10, exposing the dorsal cord surface with the dura remaining intact. The exposed spinal cord segment (approximately 3 mm in length) of the injury-saline group and the injury-XCT90 group was subjected to a moderate contusive SCI using a modified Allen's weight-drop apparatus as described previously (Chen et al., 2010). Following surgery, all animals were injected with penicillin G (4 wu, i.m.) once a day in both hindlimbs for 5 days, and their bladders were manually massaged twice daily. XCT790 (Tocris Bioscience, Bristol, UK) was prepared in 10 mM dimethyl sulfoxide (DMSO) with gentle warming, and then the solution was diluted to 1% with saline. In the injury-XCT90 group, the animals underwent a laminectomy plus traumatic SCI operation and then were injected with XCT790 intraperitoneally (0.48 mg/kg) at 30 min post-surgery and once a day until sacrifice. In the injury-saline and sham groups, the animals were subjected to similar treatment consisting of an equivalent volume of sterile saline.

Histological examination and immunohistochemical (IHC) analysis

The animals were anesthetized via an intraperitoneal injection of 10% chloral hydrate (300 mg/kg) and sacrificed by transcardial perfusion with heparinized saline for 20 min, followed by fixing with 4% paraformaldehyde in 0.1 M phosphate-buffered saline (PBS), pH 7.4. The spinal tissue spanning the injury epicenter with 5 mm of adjacent rostral and caudal segments was dissected from the spinal column, post-fixed overnight at 4 °C in 4% paraformaldehyde, and then embedded in paraffin. Paraffin sections with a 4-μm thickness were stained with hematoxylin and eosin for histological assessment and placed onto charged-glass microscope slides for IHC staining. After deparaffinization, antigen retrieval and endogenous peroxidase inactivation, the slides were incubated overnight at 4 °C with an anti-ERRα antibody (1:200 Santa Cruz Biotechnology, Santa Cruz, CA, USA) and 2% bovine serum albumin (BSA) or with PBS as a negative control for the IHC staining study. The sections were then washed and incubated with a goat anti-rabbit antibody (ready-to-use Dako REAL™ EnVision™/HRP, Danmark) for 50 min at room temperature (RT). Finally, the sections were incubated in DAB-containing Substrate Working Solution (Dako K500711, Danmark) for 10 min, rinsed in dH2O, counterstained with hematoxylin, dehydrated, and placed in mounting medium. All the sections were observed under a digital camera (Leica DM4000B, Germany) (×50 magnification). The transverse sections with the severest injury were

assigned as the lesion epicenter. Using Image-Pro Plus 6.0 (Media Cybernetics, Silver Springs, MD, USA) software, the cavity areas were outlined and quantified. Sections of the injury epicenter were analyzed and the ratio for ''cavity area/total area'' from each section determined. For quantitative analysis of the number of positive cells, two sections from the lesion epicenter of each specimen were randomly selected and three random images in the anterior horn of gray matter visual fields of each slice were obtained under digital camera (×200 magnification). Dark brown-colored neuronal cells were scored as positive for the stain and blindly counted by two examiners.

Immunofluorescence

The animals were sacrificed and perfused as described above. The dissected tissues were fixed in 4% paraformaldehyde in PBS (pH 7.4) for 3 h and maintained overnight in 6% sucrose/PBS, rinsed with acetone, and embedded in optimal cutting temperature compound (OCT) (Sakura Finetek USA, Inc., Torrance, CA, USA). The samples were stored at −80 °C until they were sectioned (10 μm), and the slides were stored at −20 °C. When ready, the slides were thawed at RT for 20 min, washed with PBS for 10 min, and blocked with 10% goat serum diluted in PBS for 1 h. The slides were then probed with a mouse monoclonal RECA-1 antibody (1:200; Abcam plc, Cambridge, UK) or rabbit monoclonal PCNA antibody (1:200; Abcam) diluted in 3% goat serum in PBS overnight at 4 °C, followed by incubation with the secondary antibodies, Alexa Fluor 488 goat anti-rabbit IgG (H + L) (1:1000, Jackson, West Grove, PA, USA) and Cy3 goat anti-mouse IgG (H + L) (1:1000, Jackson, USA), diluted in 3% goat serum for 30 min at RT. The sections were washed with PBS followed by counterstaining with 4',6-diamidino-2-phenylindole (DAPI), and then mounted using an antifade mounting medium. Visual fields in the anterior horn of gray matter were obtained using a Leica DM4000B camera (×200 magnification). Two sections from the lesion epicenter of each specimen and three fields per slide were selected at random. The evaluator was blinded to the treatments received and counted the number of RECA-1 label (red) and RECA-1/PCNA/DAPI merged label (white) manually.

Western blot

A 1-cm segment of spinal cord encompassing the injury site was harvested and immediately frozen in liquid nitrogen and stored at −80 °C until further processing. The frozen spinal cord was lysed by radio immunoprecipitation assay (RIPA) lysis buffer (50 mM Tris (pH 7.4), 150 mM NaCl, 1% Triton X-100, 1% sodium deoxycholate, 0.1% SDS, 1 mM sodium orthovanadate, 2 mM sodium fluoride, 1 mM EDTA, 0.5 μg/ml leupeptin, 0.7 μg/ml Pepstatin A, 50 μg/ml PMSF, 2.2 μg/ml Aprotinin), and protein concentrations were determined using a Bradford protein assay (Wellbio, Changsha, China). Forty micrograms of proteins were loaded and separated by SDS gel electrophoresis, and then transferred to PVDF membranes (Millipore, Mississauga, Canada). The membranes were blocked in 5% skimmed milk in Tris-buffered saline with 0.1% Tween (TBS-T) for 1 h at RT. The membranes were then incubated overnight at 4 °C with a rabbit-anti-ERRα antibody (1:500; Sigma–Aldrich, St. Louis, MO, USA), rabbit-anti-PGC-1α antibody (1:500; Santa Cruz Biotechnology), mouse-anti-VEGF antibody (1:200, Abcam) and rabbit-anti-Ang-2 antibody (1:500, Abcam), followed by incubation with horseradish peroxidase (HRP)-conjugated secondary antibodies, goat anti-rabbit IgG (H + L) (1:3000, cwbiotech, China) or goat anti-mouse IgG (H + L) (1:3000, cwbiotech, China) for 1 h at RT. Immunoreactive protein bands were visualized using an enhanced chemiluminescence detection system (Super Signal ECL Kit, Thermo Scientific, IL, USA). The relative intensities were determined using Quantity One 4.6.2 software (Bio-Rad, Hercules, CA, USA), and β-actin was used as the internal control.

Quantitative real-time polymerase chain reaction (qRT-PCR)

Total RNA from 10-mm long spinal cord segments containing the injury epicenter was extracted with TRIzol (Invitrogen, Carlsbad, CA, USA) according to the manufacturer's instructions. Single-stranded cDNA was synthesized from a total of 3-μg RNA using the RevertAid™ First Strand cDNA Synthesis Kit (Thermo Fisher Scientific, Pittsburgh, PA, USA) and qRT-PCR was performed using SYBGREEN PCR Master Mix (Applied Biosystems, Foster City, CA, USA). Tm was determined in accordance with the specificity of the melting curve after amplification. The following primers, designed and synthesized by GenScript Inc., were used with annealing temperatures of 60 °C:

ERRα:
Forward: AAGCCCTGATGGACACCTC
Reverse: GAAGCCTGGGATGCTCTTG
PGC-1α:
Forward: TGGAGCAATAAAGCAAAGAGC
Reverse: GTGTGAGGAGGGTCATCGTT
VEGF:
Forward: CTTGAGTTGGGAGGAGGATG
Reverse: TGGCAGGCAAACAGACTTC
Ang-2:
Forward: GCAAGCATACAGGAGGGTCT
Reverse: ATCAAAGTGGACAGGCAAGC
β-actin:
Forward: CATCCTGCGTCTGGACCTGG
Reverse: TAATGTCACGCACGATTTCC

The PCR reaction was performed in an ABI 7500 Real-Time PCR thermocycler (Applied Biosystems, Foster City, CA, USA). Analyses of gene expression were performed using the $2^{-\Delta\Delta Ct}$ method. Agarose gel electrophoresis showed that PCR products migrated to the expected position, validating the specificity of the primers used in the qRT-PCR (data not shown).

Statistical analysis

Statistical analysis was performed using the SPSS 17.0 software package (SPSS Inc., Chicago, IL, USA). Data

for each variable were presented as mean ± SD. Mean contrast was analyzed by Student's *t* test for comparison in the cavity area between the injury-XCT790 group and the injury-saline group. For other data, the significance between groups was evaluated using a one-way analysis of variance (ANOVA) followed by a Newman–Keuls post hoc test. $P < 0.05$ was interpreted as statistically significant during the mean difference analysis.

RESULTS

XCT790 inhibited ERRα expression and aggravated tissue damage in the injured spinal cord

Compared with the outcomes in the injury-saline and sham groups, a distinct histopathological appearance was observed 3 days post-surgery in the injury-XCT790 group. Many normal neurons were observed in the gray matter ventral horn of the uninjured (sham) spinal cord with no sign of cellular destruction (Fig. 1A). A series of histopathological changes to the spinal cord, such as inflammatory cell infiltration, hemorrhage and vacuolation, and fewer normal neurons were observed in the injury-XCT790 group (Fig. 1C) compared with the injury-saline group (Fig. 1B). Besides, the cavity areas were increased in the injury-XCT790 group compared with the injury-saline group at the injury epicenter 7 days post-surgery (Fig. 2).

Brown-colored ERRα molecules were observed in the nuclei of many cells of the uninjured spinal cord gray matter (Fig. 1D). Fewer ERRα-positive cells were observed at 1, 3 and 7 days after SCI (Fig. 1G). Both the injury-XCT790 and injury-saline groups exhibited a similar change tendency in ERRα expression, with the highest levels of ERRα observed on day 3 after traumatic SCI (Fig. 1E, F). However, XCT790 injection significantly repressed the release of ERRα at 1, 3 and 7 days post-injury (Fig. 1G). In agreement with the immunohistochemistry staining results, qRT-PCR revealed that ERRα expression in the injury-XCT790 group was significantly decreased compared with the injury-saline group on day 1, 3 and 7 after SCI (Fig. 4A). Moreover, the protein levels of ERRα in the injury-XCT790 group were also significantly lower throughout the experiment (Fig. 3A).

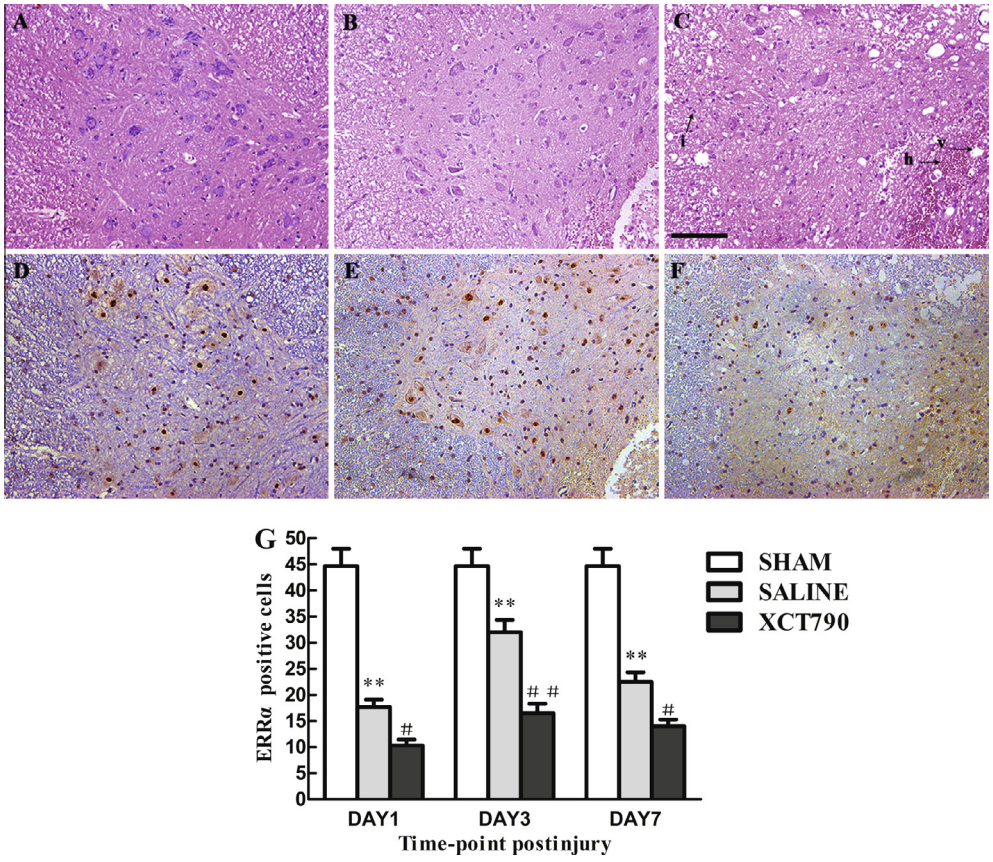

Fig. 1. Effects of XCT790 on the histopathological features and ERRα expression in the ventral horn of the injured spinal cord site according to H&E and immunohistochemical analyses at 1, 3 and 7 days after SCI. (A–F) Representative micrographs of the gray matter ventral horn showing differences in histopathological analysis and ERRα expression among the sham group, the injury-saline group and the injury-XCT790 group at 3 days post-injury (A&D: Sham group; B&E: injury-saline group; C&F: injury-XCT790 group, ×200 magnification). (G) Spatiotemporal comparison of the number of cells expressing ERRα among the three groups. i arrow: inflammatory cell infiltration; h arrow: hemorrhage; v arrow: vacuolation. The results are expressed as mean ± SD of five animals per group. Significance of the differences between groups at specific time points were evaluated using the ANOVA followed by the Newman–Keuls post hoc test ($^{*}p < 0.05$, $^{**}p < 0.01$ vs. the sham group; $^{\#}p < 0.05$, $^{\#\#}p < 0.01$ vs. the injury-saline group). Scale bar = 100 μm.

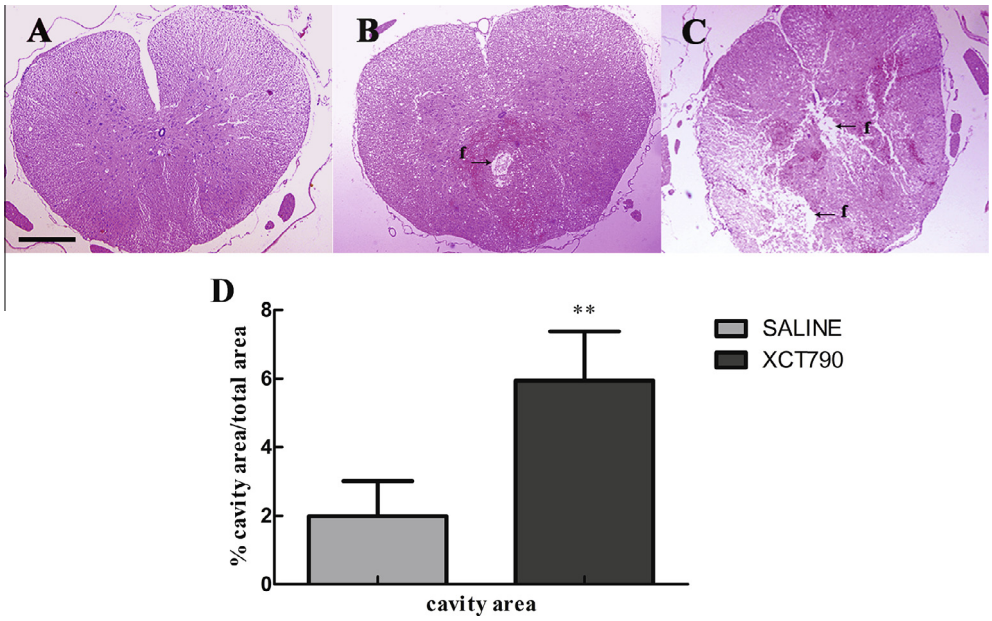

Fig. 2. Effects of XCT790 on the cavity formation in the lesion epicenter of the injured spinal cord at 7 days after SCI. Representative micrographs of the transverse section showing differences in cavity areas among the sham group, the injury-saline group and the injury-XCT790 group at 7 days post-injury (A: Sham group; B: injury-saline group; C: injury-XCT790 group, ×50 magnification). (D) Graphical representation showing a statistically significant increase in cavity areas following XCT790 injection. f arrow: cavity formation. The results are expressed as mean ± SD of five animals per group. Significance of the differences between the injury-saline group and the injury-XCT790 group were analyzed by Student's *t* test (**$p < 0.01$ vs. the injury-saline group). Scale bar = 400 μm.

Inhibition of ERRα influences the expression of PGC-1α, VEGF and Ang-2 after SCI

We used Western blot analysis to evaluate changes in PGC-1α, VEGF and Ang-2 protein levels at the lesion site. Additionally, qRT-PCR was applied to detect expression of these genes at various time points after SCI, from 24 h to 7 days. The western blot results revealed that PGC-1α protein expression in injury-saline-treated animals was significantly lower at 1 day after SCI, and then was increased to the peak at 3 days after SCI, followed by a remarkable decline at 7 days after SCI compared to sham animals. Data analysis indicates that PGC-1α protein expression in the injury-XCT790 group was not repressed as compared to that in the injury-saline group at 1 day after trauma but was reduced by 3 and 7 days after SCI (Fig. 3B). Moreover, qRT-PCR analyses revealed that PGC-1α gene expression between the injury-XCT790 group and the injury-saline group had no significant statistical difference at all time points (Fig. 4B). We also found that SCI induced a significant increase in VEGF protein levels 24 h after SCI, relative to sham animals that remain elevated until 7 days post-injury. Nevertheless, compared with the injury-saline group, inhibition of ERRα in the injury-XCT790 group significantly reverted the upregulation of VEGF induced by the injury at 1 day post injury and repressed expression even more at 3 and 7 days (Fig. 3C). This significant reduction in VEGF in the injury-XCT790 group was further validated by the qRT-PCR results (Fig. 4C). It is worth noting that a marked decrease in Ang-2 protein levels was observed 1 day after SCI in the injury-saline group. However, starting on day 3 after SCI, Ang-2 levels gradually began to increase over time. Quantitative analysis of Ang-2 levels in both the injury-XCT790 and injury-saline groups indicated that the decrease in Ang-2 protein levels was significant at all time points (Fig. 3D). These results were further confirmed by those of the qRT-PCR analysis (Fig. 4D).

Reduced ERRα expression decreased vascular density and endothelial cell proliferation after SCI

To determine whether SCI was responsible for the change in vascular density and whether the spinal cord vasculature was actively proliferating after SCI in the various groups, tissue slices of 1, 3 and 7 days after SCI were stained with antibodies against the endothelial cell marker RECA-1 and against a marker of proliferating cells, PCNA. RECA-1 immunofluorescence revealed a significant decrease in the number of vessels at 24 h post-injury compared with those of the uninjured (sham) animals. At 3 and 7 days after SCI, the density of RECA-1-labeled blood vessels in the injury-XCT790 and injury-saline groups gradually increased and reached a peak 7 days after SCI (Fig. 5B, C). However, significant differences between the injury-XCT790 and injury-saline groups were observed at 1, 3 and 7 days after SCI (Fig. 5D). We quantified the number of proliferating endothelial cells (RECA-1/PCNA) to assess angiogenesis (Fig. 6A). Uninjured spinal cord tissue showed relatively low basal levels of endothelial cell proliferation. However, sections from the injury-saline group 3 and 7 days after SCI exhibited a significant number of proliferating endothelial cells in angiogenic

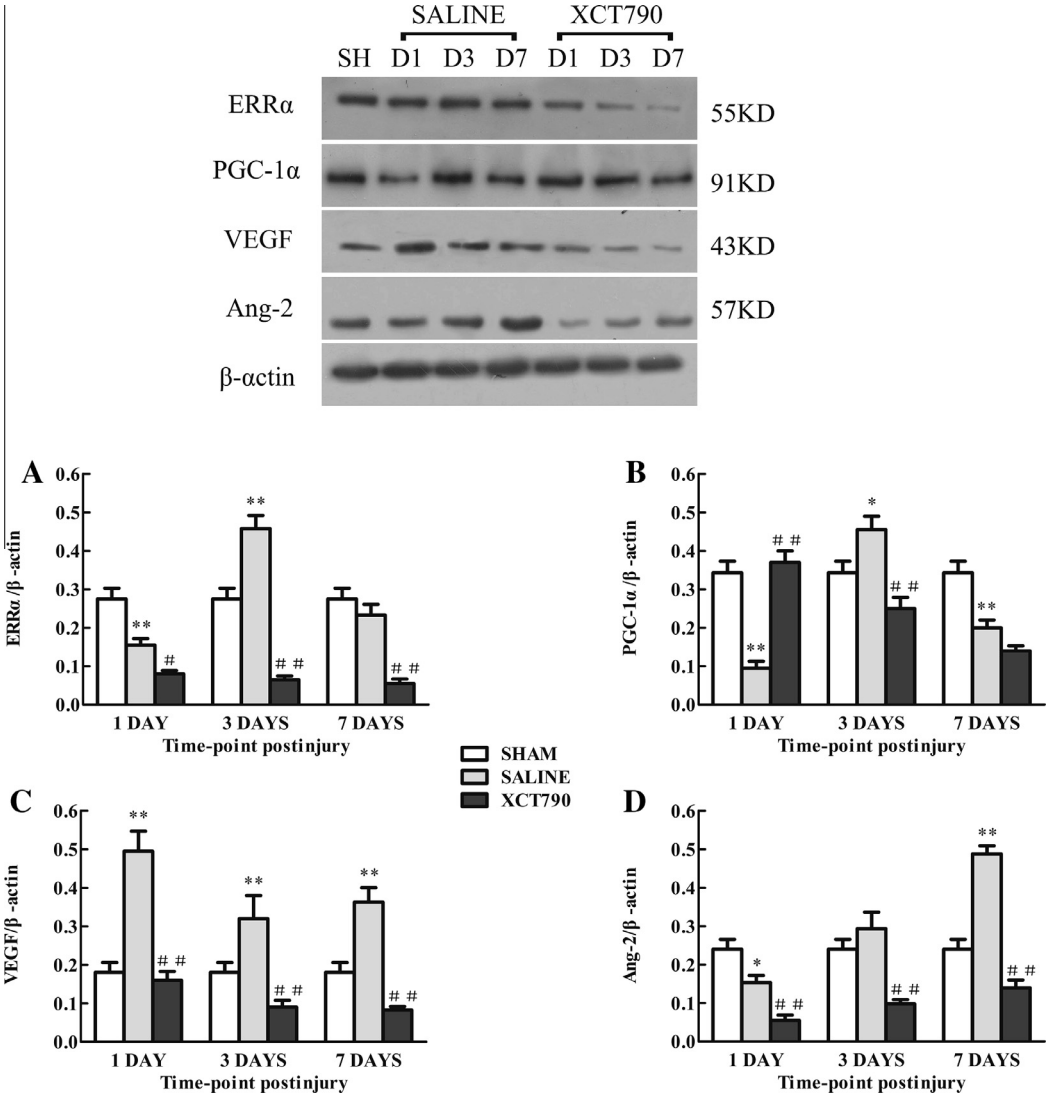

Fig. 3. Effects of XCT790 on the protein expression of ERRα, PGC-1α, VEGF and Ang-2 at 1, 3 and 7 days after SCI. Western blot bands show the protein expression levels of ERRα, PGC-1α, VEGF and Ang-2 at various time points after SCI in each group (n = 5). (A–D) Comparison of ERRα, PGC-1α, VEGF and Ang-2 protein expression among the three groups (n = 5) at various time points after SCI. Data represent mean ± SD, and significance of the differences between groups at specific time points were evaluated using the ANOVA followed by the Newman–Keuls post hoc test ($^{*}p < 0.05$, $^{**}p < 0.01$ vs. the sham group; $^{\#}p < 0.05$, $^{\#\#}p < 0.01$ vs. the injury-saline group).

vessels. XCT790 injection significantly reduced the number of proliferating endothelial cells compared with those of the injury-saline group 3 and 7 days after SCI (Fig. 6B).

DISCUSSION

Traumatic SCI causes an immediate loss of vascular supply and initiates a multifaceted response to injury. A loss of blood vessels causes cell death and a loss of tissue integrity. Therefore, early reconstruction of blood vessels could support the repair of the injured spinal cord (Ning et al., 2013). Angiogenesis is a highly synchronized and tightly regulated process that involves endothelial cell proliferation, migration, vascular tubule formation and cell survival, and it requires stringent orchestration by the tissue being vascularized (Fong, 2008; Sapieha, 2012).

To date, few studies have revealed a role for ERRα in the process of angiogenesis after SCI. In fact, to our knowledge, this is the first study to investigate whether XCT790 antagonizes ERRα expression and its effects on PGC-1α, VEGF, and Ang-2 expression, vascular density and endothelial cell proliferation in an experimental rat model of traumatic SCI. Taken together, the present results indicate that XCT790 injection significantly suppressed expression of ERRα, thus down-regulating expression of VEGF and Ang-2, decreasing vessel density and reducing endothelial cell proliferation. An attenuation of ERRα accumulation might inhibit angiogenesis following rat SCI compared with changes observed in the injury-saline group.

ERRα has shown to function as a regulator of oxidative metabolism across a wide range of tissues (Huss et al., 2004; Bonnelye et al., 2007; Stein et al., 2008; Xue et al., 2009; Ndubuizu et al., 2010). Our study

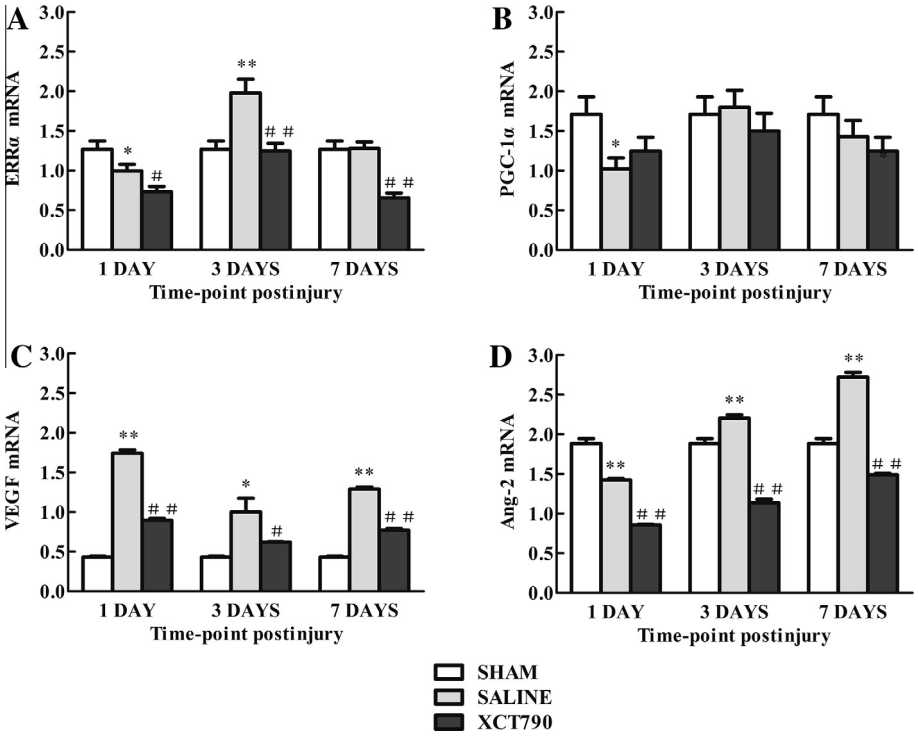

Fig. 4. Effects of XCT790 on the expression of ERRα, PGC-1α, VEGF and Ang-2 mRNA at 1, 3 and 7 days after SCI. (A–D) Comparison of ERRα mRNA, PGC-1α mRNA, VEGF mRNA and Ang-2 mRNA expression among the three groups ($n = 5$) at various time points after SCI. Data represent mean ± SD, and significance of the differences between groups at specific time points were evaluated using the ANOVA followed by the Newman–Keuls post hoc test ($^{*}p < 0.05$, $^{**}p < 0.01$ vs. the sham group; $^{\#}p < 0.05$, $^{\#\#}p < 0.01$ vs. the injury-saline group).

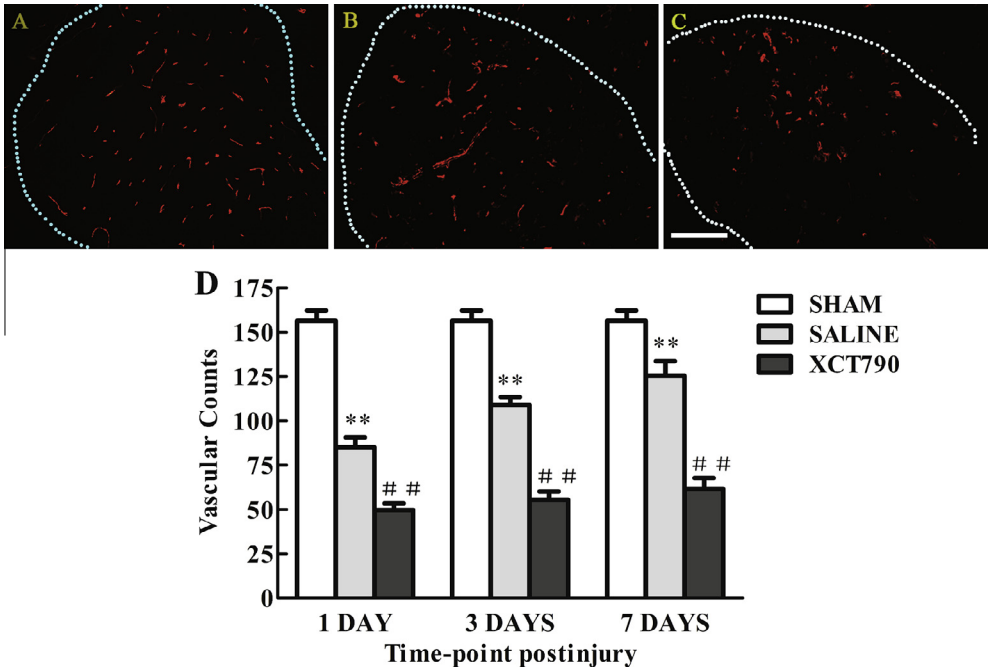

Fig. 5. Effects of XCT790 on vascular density in the injured spinal cord site at 1, 3 and 7 days after SCI. Representative images taken from the ventral horn of the spinal cord at 7 days post-injury. The vessels were labeled with RECA-1 (A: Sham group; B: injury-saline group; C: injury-XCT790 group, ×200 magnification). (D) Spatiotemporal comparison of RECA-1 labeled vascular counts among the three groups. Data represent mean ± SD of five animals per group, and significance of the differences between groups at specific time points were evaluated using the ANOVA followed by the Newman–Keuls post hoc test ($^{*}p < 0.05$, $^{**}p < 0.01$ vs. the sham group; $^{\#}p < 0.05$, $^{\#\#}p < 0.01$ vs. the injury-saline group). Scale bar = 100 μm.

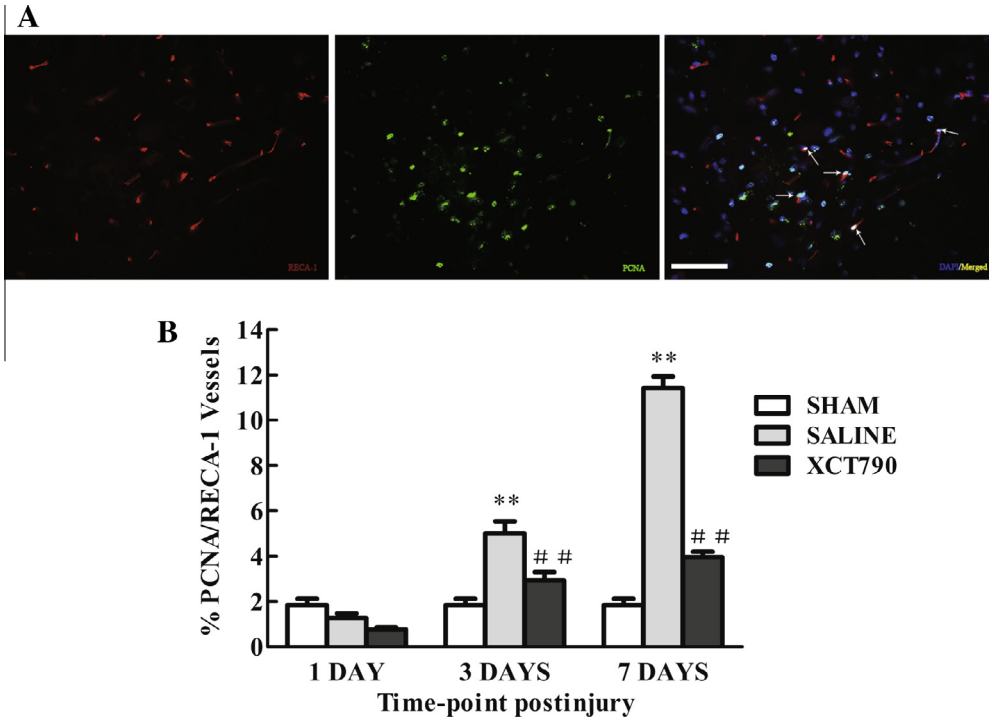

Fig. 6. Effects of XCT790 on vascular endothelial cell proliferation in the injured spinal cord site at 1, 3 and 7 days after SCI. (A) Representative PCNA/RECA-1 double-labeled images (RECA-1, red; PCNA, green; DAPI, blue, ×200 magnification) taken from the ventral horn of the spinal cord at 7 days post-injury. White arrowheads indicate the merged labeling, which represents vascular proliferation. (B) Spatiotemporal comparison of proliferative vascular endothelial cells among the three groups. Data represent mean ± SD of five animals per group, and significance of the differences between groups at specific time points were evaluated using the ANOVA followed by the Newman–Keuls post hoc test ($^{*}p < 0.05$, $^{**}p < 0.01$ vs. the sham group; $^{\#}p < 0.05$, $^{\#\#}p < 0.01$ vs. the injury-saline group). Scale bar = 100 μm.

found that ERRα mostly localizes to the nucleus of the spinal cord gray matter. Estrogen-related receptors (ERRs) are a family of orphan nuclear hormone receptors initially identified based on their homology to the estrogen receptor ERα. ERα and ERRα bind to and activate transcription through the classical estrogen response element (ERE) (Vanacker et al., 1999). A recent paper has demonstrated that ERα was up-regulated after SCI and the activation of this receptor mediates some of the functional locomotor recovery and the extent of white matter spared tissue (Mosquera et al., 2014). According to the histopathological and protein expression results, we found that the number of ERRα-positive cells was lower, but the protein expression of ERRα was higher 3 days after SCI and similar 7 days after SCI. We surmise that the primary insult after SCI caused immediate tissue structural destruction, thereby reducing the number of cells that express ERRα. ERRα is not a constitutively active receptor and that transformation into an active form is favored by binding to PGC-1α. High metabolic needs after SCI regulated the expression of PGC-1α and thus may affect the activity of ERRα (Schreiber et al., 2003). Subsequently, a cascade of biochemical and cellular processes was involved in the spinal cord secondary injury that triggered an upregulation of the ERRα protein expression to support the high metabolic needs that characterize highly proliferative endothelial cells. The concomitant induction of angiogenesis by ERRα, therefore, serves to supplement the limited oxygen and nutrient supply provided by existing vessels (Stein et al., 2009). Oxygen and nutrient supply is conducive to tissue repair and minimizing nerve damage after SCI. With the gradual increase of karyolysis and vacuolation, the number of ERRα-positive cells and the protein expression of ERRα declined 7 days after SCI. Further research is required to elucidate the mechanism underlying the ERRα activation and identify which cells from the CNS express ERRα. XCT790 significantly repressed the expression of ERRα, thereby decreasing the metabolic rate and cellular oxygen supply, which ultimately resulted in an attenuation of cellular repair. In agreement with the IHC staining results, the expression of ERRα mRNA and protein decreased 24 h after SCI, increased to peak levels on day 3, and dropped on day 7. Our results also demonstrated that XCT790 intervention significantly repressed the expression of ERRα protein and mRNA throughout the whole period.

PGC-1α is dramatically induced by nutrient and oxygen deprivation and, in turn, regulates a varied suite of genes involved in the coordination of neovascularization (Arany et al., 2008). PGC-1α is highly versatile and has the ability to co-activate many different transcriptional factors, including nuclear respiratory factors (NRF-1 and NRF-2), estrogen-related receptor-α, Gabpa/b, PPARs, and the thyroid hormone receptor (Zheng et al., 2010). PGC-1α interacts directly with the basal transcriptional machinery and also

recruits chromatin-modifying enzymes, such as histone acetylase p300, to open chromatin and facilitate transcription (Shoag and Arany, 2010). The addition of PGC-1α to the orphan nuclear receptor ERRα led to an eightfold induction of luciferase activity (Arany et al., 2008). VEGF and Ang-2 was induced in muscle creatine kinase–PGC-1α transgenic animals (Arany et al., 2008). PGC-1α coactivates ERRα on a number of sites found both in the promoter and a novel conserved enhancer located in the first intron of the VEGF gene as demonstrated by chromatin immunoprecipitation assays (Shoag and Arany, 2010). Consistent with the ability of PGC-1α to induce ERRα activity and expression, PGC-1α and ERRα show similar spatial and temporal expression patterns in vivo (Herzog et al., 2006). Previous research has shown that ERRα can function as a specific molecular repressor of PGC-1α activity and can dramatically and specifically repress PGC-1α transcriptional activity (Ichida et al., 2002). Recent studies have found that ERRα partially regulates PGC-1α expression and coordinates with PGC-1α to mediate mitochondrial biogenesis (Handschin et al., 2003; Wang et al., 2010). In the present study, we observed that the injury-saline groups exhibited a similar change in PGC-1α and ERRα expression after acute SCI. However, inhibition of ERRα was not able to significantly repress PGC-1α protein and mRNA expression, compared with those of the injury-saline group.

Angiogenesis and neurogenesis that take place in the secondary and chronic phase after SCI and neuronal protection that is impaired in the acute phase post-injury (Herrera et al., 2009). VEGF can improve microcirculation during early stages of SCI and regenerate blood vessels during the late reconstruction stage of SCI via angiogenesis (Herrera et al., 2009; Zhou et al., 2013; Liu et al., 2014). Moreover, some research has shown the neuroprotective effect of VEGF in attenuating axonal degradation and leads to better locomotor recovery following SCI (Herrera et al., 2009; Liu et al., 2010; Yamaya et al., 2014). The induction in VEGF expression was mediated, at least in part, by activation of the ERR pathway (Zhang et al. (2011)). It is likely that ERRα is able to activate the VEGF promoter directly through the ERRE (Stein et al., 2009). Spiegleman and colleagues examined the murine VEGF promoter to show that the induction of angiogenesis is a result of direct transcriptional regulation of VEGF by ERRα (Arany et al., 2008). In our present study, VEGF was present at low levels in normal spinal cord tissue; SCI induced a significant elevation in expression until day 7, with peak expression levels reached 24 h following SCI. However, XCT790 injection dramatically reduced the expression of VEGF throughout the course of recovery. The expression profiles of the ERRα and VEGF proteins and mRNAs are very similar in the injury groups suggesting the induction of angiogenesis is a result of direct transcriptional regulation of VEGF by ERRα after SCI. In the injured CNS, VEGF predominantly binds to the tyrosine kinase receptor flk-1 (KDR/VEGF-R2) that is expressed on the vascular endothelium and some neurons and by triggering the mitotic and migratory processes necessary for angiogenesis (Krum et al., 2008). Some research has shown that VEGF and its receptor mRNAs and proteins are induced and slightly upregulated within 1 day in rats with a contusion injury and persisted for at least 14 days (Skold et al., 2000; Choi et al., 2007). Hence, we should further explore the effect of ERRα on VEGF receptors in our next research.

Ang-2 can be induced mainly by COX-2 enzymatic activity and is expressed by endothelial cells at sites of active angiogenesis (Pichiule et al., 2004; Ng et al., 2011). Upon release from endothelial cells, Ang-2 exerts autocrine and paracrine effects on the Tie-2 receptor, thereby antagonizing Ang-1's effect on vascular integrity in injured spinal cords (Durham-Lee et al., 2012). A sufficient level of VEGF is present after endothelial cell growth, proliferation, and Ang-2-induced angiogenic sprouting, which leads to angiogenesis. Recent research found that Ang-2 mRNA and protein levels are up-regulated up to 10 weeks after SCI, which may underlie the early angiogenic response following the loss of blood vessels that occurs within 3–7 days (Ritz et al., 2010; Durham-Lee et al., 2012). Previous studies have shown that Ang-2 can be induced by the adenoviral delivery of PGC-1α to the primary skeletal muscle (Arany et al., 2008). However, this study did not address whether ERRα inhibition affected the expression of Ang-2. Our research found that Ang-2 mRNA and protein levels significantly decreased 1 day after SCI, then rapidly increased until day 7. Inhibition of ERRα expression significantly decreased the mRNA and protein levels of Ang-2 throughout the whole period. The expression profile of the ERRα, VEGF and Ang-2 proteins and mRNAs are very similar in the injury groups, the mechanism by which ERRα and/or VEGF regulate the expression of Ang-2 and Tie-2 after SCI should be further probed.

Most endothelial cells undergo oncosis and death during the first 24 h after SCI, which can largely be attributed to the initial mechanical damage (Casella et al., 2006). Subsequently, vessel density continued to decrease until the next day, with little or no observable vessels at the lesion epicenter (Casella et al., 2002). Robust angiogenesis, which results in increasing vascular density, was observed as early as 3 days after SCI and persisted as long as 1 week after SCI, with maximal endothelial cell proliferation observed 7 days post-injury (Loy et al., 2002; Figley et al., 2014). Our findings were consistent with other research in the field, demonstrating that significant angiogenesis occurred between 3 and 7 days after SCI. XCT790 decreased vascular density and endothelial cell proliferation, thereby significantly inhibiting angiogenesis at 3 and 7 days after SCI.

CONCLUSION

XCT790 significantly inhibited the expression of ERRα, resulting in a decrease in VEGF and Ang-2 expression and a reduction in the vascular density and endothelial cell proliferation in a rat traumatic SCI model. ERRα was also involved in mediating angiogenesis after SCI in this model.

Acknowledgments—This work was supported by grants from the National Natural Science Foundation of China (No. 81171698 and

No. 81371956), and from Specialized Research Fund for the Doctoral Program of Higher Education (No. 20130162110078).

REFERENCES

Amar AP, Levy ML (1999) Pathogenesis and pharmacological strategies for mitigating secondary damage in acute spinal cord injury. Neurosurgery 44(1027–1039):1039–1040.

Arany Z, Foo SY, Ma Y, Ruas JL, Bommi-Reddy A, Girnun G, Cooper M, Laznik D, Chinsomboon J, Rangwala SM, Baek KH, Rosenzweig A, Spiegelman BM (2008) HIF-independent regulation of VEGF and angiogenesis by the transcriptional coactivator PGC-1alpha. Nature 451:1008–1012.

Bazley FA, Hu C, Maybhate A, Pourmorteza A, Pashai N, Thakor NV, Kerr CL, All AH (2012) Electrophysiological evaluation of sensory and motor pathways after incomplete unilateral spinal cord contusion. J Neurosurg Spine 16:414–423.

Bianco S, Lanvin O, Tribollet V, Macari C, North S, Vanacker JM (2009) Modulating estrogen receptor-related receptor-alpha activity inhibits cell proliferation. J Biol Chem 284:23286–23292.

Bonnelye E, Zirngibl RA, Jurdic P, Aubin JE (2007) The orphan nuclear estrogen receptor-related receptor-alpha regulates cartilage formation in vitro: implication of Sox9. Endocrinology 148:1195–1205.

Casella GT, Bunge MB, Wood PM (2006) Endothelial cell loss is not a major cause of neuronal and glial cell death following contusion injury of the spinal cord. Exp Neurol 202:8–20.

Casella GT, Marcillo A, Bunge MB, Wood PM (2002) New vascular tissue rapidly replaces neural parenchyma and vessels destroyed by a contusion injury to the rat spinal cord. Exp Neurol 173:63–76.

Chen C, Chen Q, Mao Y, Xu S, Xia C, Shi X, Zhang JH, Yuan H, Sun X (2010) Hydrogen-rich saline protects against spinal cord injury in rats. Neurochem Res 35:1111–1118.

Choi JS, Kim HY, Cha JH, Choi JY, Park SI, Jeong CH, Jeun SS, Lee MY (2007) Upregulation of vascular endothelial growth factor receptors Flt-1 and Flk-1 following acute spinal cord contusion in rats. J Histochem Cytochem 55:821–830.

Distler JH, Hirth A, Kurowska-Stolarska M, Gay RE, Gay S, Distler O (2003) Angiogenic and angiostatic factors in the molecular control of angiogenesis. Q J Nucl Med 47:149–161.

Dore-Duffy P, LaManna JC (2007) Physiologic angiodynamics in the brain. Antioxid Redox Signal 9:1363–1371.

Dray C, Rougon G, Debarbieux F (2009) Quantitative analysis by in vivo imaging of the dynamics of vascular and axonal networks in injured mouse spinal cord. Proc Natl Acad Sci U S A 106:9459–9464.

Durham-Lee JC, Wu Y, Mokkapati VU, Paulucci-Holthauzen AA, Nesic O (2012) Induction of angiopoietin-2 after spinal cord injury. Neuroscience 202:454–464.

Figley SA, Khosravi R, Legasto JM, Tseng YF, Fehlings MG (2014) Characterization of vascular disruption and blood-spinal cord barrier permeability following traumatic spinal cord injury. J Neurotrauma 31:541–552.

Fong GH (2008) Mechanisms of adaptive angiogenesis to tissue hypoxia. Angiogenesis 11:121–140.

Handschin C, Rhee J, Lin J, Tarr PT, Spiegelman BM (2003) An autoregulatory loop controls peroxisome proliferator-activated receptor gamma coactivator 1alpha expression in muscle. Proc Natl Acad Sci U S A 100:7111–7116.

Herrera JJ, Nesic O, Narayana PA (2009) Reduced vascular endothelial growth factor expression in contusive spinal cord injury. J Neurotrauma 26:995–1003.

Herzog B, Cardenas J, Hall RK, Villena JA, Budge PJ, Giguere V, Granner DK, Kralli A (2006) Estrogen-related receptor alpha is a repressor of phosphoenolpyruvate carboxykinase gene transcription. J Biol Chem 281:99–106.

Huss JM, Torra IP, Staels B, Giguere V, Kelly DP (2004) Estrogen-related receptor alpha directs peroxisome proliferator-activated receptor alpha signaling in the transcriptional control of energy metabolism in cardiac and skeletal muscle. Mol Cell Biol 24:9079–9091.

Ichida M, Nemoto S, Finkel T (2002) Identification of a specific molecular repressor of the peroxisome proliferator-activated receptor gamma Coactivator-1 alpha (PGC-1alpha). J Biol Chem 277:50991–50995.

Krum JM, Mani N, Rosenstein JM (2008) Roles of the endogenous VEGF receptors flt-1 and flk-1 in astroglial and vascular remodeling after brain injury. Exp Neurol 212:108–117.

Lanvin O, Bianco S, Kersual N, Chalbos D, Vanacker JM (2007) Potentiation of ICI182,780 (Fulvestrant)-induced estrogen receptor-alpha degradation by the estrogen receptor-related receptor-alpha inverse agonist XCT790. J Biol Chem 282:28328–28334.

Liu X, Zhou Y, Wang Z, Yang J, Gao C, Su Q (2014) Effect of VEGF and CX43 on the promotion of neurological recovery by hyperbaric oxygen treatment in spinal cord-injured rats. Spine J 14:119–127.

Liu Y, Figley S, Spratt SK, Lee G, Ando D, Surosky R, Fehlings MG (2010) An engineered transcription factor which activates VEGF-A enhances recovery after spinal cord injury. Neurobiol Dis 37:384–393.

Long HQ, Li GS, Hu Y, Wen CY, Xie WH (2012) HIF-1alpha/VEGF signaling pathway may play a dual role in secondary pathogenesis of cervical myelopathy. Med Hypotheses 79:82–84.

Loy DN, Crawford CH, Darnall JB, Burke DA, Onifer SM, Whittemore SR (2002) Temporal progression of angiogenesis and basal lamina deposition after contusive spinal cord injury in the adult rat. J Comp Neurol 445:308–324.

Lutton C, Young YW, Williams R, Meedeniya AC, Mackay-Sim A, Goss B (2012) Combined VEGF and PDGF treatment reduces secondary degeneration after spinal cord injury. J Neurotrauma 29:957–970.

Mosquera L, Colon JM, Santiago JM, Torrado AI, Melendez M, Segarra AC, Rodriguez-Orengo JF, Miranda JD (2014) Tamoxifen and estradiol improved locomotor function and increased spared tissue in rats after spinal cord injury: their antioxidant effect and role of estrogen receptor alpha. Brain Res 1561:11–22.

Ndubuizu OI, Tsipis CP, Li A, LaManna JC (2010) Hypoxia-inducible factor-1 (HIF-1)-independent microvascular angiogenesis in the aged rat brain. Brain Res 1366:101–109.

Ng MT, Stammers AT, Kwon BK (2011) Vascular disruption and the role of angiogenic proteins after spinal cord injury. Transl Stroke Res 2:474–491.

Ning G, Tang L, Wu Q, Li Y, Li Y, Zhang C, Feng S (2013) Human umbilical cord blood stem cells for spinal cord injury: early transplantation results in better local angiogenesis. Regen Med 8:271–281.

Pichiule P, Chavez JC, LaManna JC (2004) Hypoxic regulation of angiopoietin-2 expression in endothelial cells. J Biol Chem 279:12171–12180.

Pichiule P, LaManna JC (1985) Angiopoietin-2 and rat brain capillary remodeling during adaptation and deadaptation to prolonged mild hypoxia. J Appl Physiol (1985) 93:1131–1139.

Ritz MF, Graumann U, Gutierrez B, Hausmann O (2010) Traumatic spinal cord injury alters angiogenic factors and TGF-beta1 that may affect vascular recovery. Curr Neurovasc Res 7:301–310.

Sapieha P (2012) Eyeing central neurons in vascular growth and reparative angiogenesis. Blood 120:2182–2194.

Schreiber SN, Knutti D, Brogli K, Uhlmann T, Kralli A (2003) The transcriptional coactivator PGC-1 regulates the expression and activity of the orphan nuclear receptor estrogen-related receptor alpha (ERRalpha). J Biol Chem 278:9013–9018.

Shoag J, Arany Z (2010) Regulation of hypoxia-inducible genes by PGC-1 alpha. Arterioscler Thromb Vasc Biol 30:662–666.

Skold M, Cullheim S, Hammarberg H, Piehl F, Suneson A, Lake S, Sjogren A, Walum E, Risling M (2000) Induction of VEGF and VEGF receptors in the spinal cord after mechanical spinal injury and prostaglandin administration. Eur J Neurosci 12:3675–3686.

Stein RA, Chang CY, Kazmin DA, Way J, Schroeder T, Wergin M, Dewhirst MW, McDonnell DP (2008) Estrogen-related receptor

alpha is critical for the growth of estrogen receptor-negative breast cancer. Cancer Res 68:8805–8812.
Stein RA, Gaillard S, McDonnell DP (2009) Estrogen-related receptor alpha induces the expression of vascular endothelial growth factor in breast cancer cells. J Steroid Biochem Mol Biol 114:106–112.
Teyssier C, Bianco S, Lanvin O, Vanacker JM (2008) The orphan receptor ERRalpha interferes with steroid signaling. Nucleic Acids Res 36:5350–5361.
Vanacker JM, Pettersson K, Gustafsson JA, Laudet V (1999) Transcriptional targets shared by estrogen receptor- related receptors (ERRs) and estrogen receptor (ER) alpha, but not by ERbeta. EMBO J 18:4270–4279.
Villena JA, Kralli A (2008) ERRalpha: a metabolic function for the oldest orphan. Trends Endocrinol Metab 19:269–276.
Wang J, Wang Y, Wong C (2010) Oestrogen-related receptor alpha inverse agonist XCT-790 arrests A549 lung cancer cell population growth by inducing mitochondrial reactive oxygen species production. Cell Prolif 43:103–113.
Willy PJ, Murray IR, Qian J, Busch BB, Stevens WJ, Martin R, Mohan R, Zhou S, Ordentlich P, Wei P, Sapp DW, Horlick RA, Heyman RA, Schulman IG (2004) Regulation of PPARgamma coactivator 1alpha (PGC-1alpha) signaling by an estrogen-related receptor alpha (ERRalpha) ligand. Proc Natl Acad Sci U S A 101:8912–8917.
Xue Y, Petrovic N, Cao R, Larsson O, Lim S, Chen S, Feldmann HM, Liang Z, Zhu Z, Nedergaard J, Cannon B, Cao Y (2009) Hypoxia-independent angiogenesis in adipose tissues during cold acclimation. Cell Metab 9:99–109.
Yamaya S, Ozawa H, Kanno H, Kishimoto KN, Sekiguchi A, Tateda S, Yahata K, Ito K, Shimokawa H, Itoi E (2014) Low-energy extracorporeal shock wave therapy promotes vascular endothelial growth factor expression and improves locomotor recovery after spinal cord injury. J Neurosurg:1–12.
Zhang K, Lu J, Mori T, Smith-Powell L, Synold TW, Chen S, Wen W (2011) Baicalin increases VEGF expression and angiogenesis by activating the ERR{alpha}/PGC-1{alpha} pathway. Cardiovasc Res 89:426–435.
Zheng Z, Chen H, Wang H, Ke B, Zheng B, Li Q, Li P, Su L, Gu Q, Xu X (2010) Improvement of retinal vascular injury in diabetic rats by statins is associated with the inhibition of mitochondrial reactive oxygen species pathway mediated by peroxisome proliferator-activated receptor gamma coactivator 1alpha. Diabetes 59:2315–2325.
Zhou Y, Liu XH, Qu SD, Yang J, Wang ZW, Gao CJ, Su QJ (2013) Hyperbaric oxygen intervention on expression of hypoxia-inducible factor-1alpha and vascular endothelial growth factor in spinal cord injury models in rats. Chin Med J (Engl) 126:3897–3903.

(Accepted 29 January 2015)
(Available online 7 February 2015)